Applied Materials Today 5 (2016) 1–8

Contents lists available at ScienceDirect

Applied Materials Today

journal homepage: www.elsevier.com/locate/apmt

Nitrogen-doped mesoporous carbon thin film for binder-free supercapacitor

Pan Hu[a], Donghui Meng[b], Guohua Ren[b], Rongxin Yan[b], Xinsheng Peng[a,*]

[a] State Key Laboratory of Silicon Materials, Department of Materials Science and Engineering, Zhejiang University, Hangzhou 310028, China
[b] Beijing Institute of Spacecraft Environment Engineering, Beijing 100094, China

ARTICLE INFO

Article history:
Received 13 June 2016
Received in revised form 1 August 2016
Accepted 2 August 2016

Keywords:
Nitrogen-doped mesoporous carbon
Thin film
Binder-free
Supercapacitor

ABSTRACT

Free-standing nitrogen-doped mesoporous carbon films were successfully prepared by carbonizing gelatin/HKUST-1 composite films, which converted from gelatin/copper hydroxide nanostrands composite films. Gelatin provides the sources of both carbon and nitrogen. The formation of HKUST-1 crystals expanded the gelatin matrix and produced porous structures which were reserved during the carbonization process. The mesoporous structures of the prepared carbon film were easily wetted by electrolytes and more suitable for rapid ionic migration. This mesoporous nitrogen-doped carbon film was explored as a binder-free electrode for supercapacitor, which exhibited highest specific energy of 28.1 W h kg^{-1}, specific capacity of 316 F g^{-1} at a current density of 0.5 A g^{-1}, 168 F g^{-1} at a current density of 5 A g^{-1}, and high capacitance retention of 92.9% with degrading of 0.00064% after charging/discharging 11,000 cycles.

1. Introduction

Porous carbon materials are of great importance and promising applications in electrode materials [1–5]. Various methods have been developed to synthesize porous carbons, including chemical vapour decomposition, laser ablation, chemical or physical activation, carbonization of polymer aerogels, carbide-derived carbon, template procedures [6–10]. Besides the high surface area and porosity, pseudocapacitance also contributed to the specific capacitance. Doping nitrogen (N) into carbon material has been an effective way to enhance the electrochemical performance, mainly due to the extra faradaic redox reactions, and the strong electron donor behavior of nitrogen, and strengthening the wettability of the interface between the electrolyte and electrodes [11–15]. In most cases, nitrogen-containing carbon materials have been achieved through reaction with nitrogen-containing reagents [16,17]. However, the post-treatment processing (such as treating with NH_3 gas) generally leads to low nitrogen content. This drawback might be overcome by carbonization of nitrogen-rich carbon precursors [18].

Gelatin, a low cost and abundant fibrous and nitrogen-rich protein, is expected to be an ideal precursor for the synthesis of nitrogen-doped carbon for supercapacitor [19,20]. In order to further enhance the performance, harsh activation processes were explored. Very recently, gelatin has been carbonized to carbon by using SBA-15, and sepiolite as templates, respectively [21–23]. However, most of the prepared nitrogen-doped carbons were in powder form. Typically, non-electrochemical active binders are requested to assemble them into electrodes for supercapacitors. This could result in less active materials loading and lower power density. In addition for thin film like electronic devices, free-standing binder-free thin films electrodes are highly demanded. Up to date, free-standing mesoporous nitrogen-doped carbon thin film for binder-free supercapacitor electrode has scarcely reported.

Herein, we demonstrate a novel way for the synthesis of free-standing mesoporous nitrogen-doped carbon films (mp-NCF) through carbonizing gelatin/HKUST-1 porous composite film without activation process. The gelatin/HKUST-1 film was prepared by reacting gelatin/copper hydroxide nanostrands (CHNs) thin film with H_3BTC at room temperature. Because of the growth of HKUST-1 crystals, the compacted gelatin/CHNs film (about 1 μm thick) was converted to 4.8 μm thick and porous gelatin/HKUST-1 thin film. After carbonization under argon at different temperature and removing away the remained copper particles, free-standing mesoporous nitrogen-doped carbon film was obtained and used as binder-free electrode for supercapacitor. It shows 168 F g^{-1} at current density of 5 A g^{-1} and retained 156.2 F g^{-1} after cycling 11,000 cycles with 0.00064% degradation per cycles.

2. Experimental

2.1. Materials

Gelatin and 1,3,5-benzenetricarboxylic acid (BTC) were purchased from Sigma–Aldrich. The gelatin was generated from pork

* Corresponding author.
E-mail address: pengxinsheng@zju.edu.cn (X. Peng).

http://dx.doi.org/10.1016/j.apmt.2016.08.001
2352-9407/

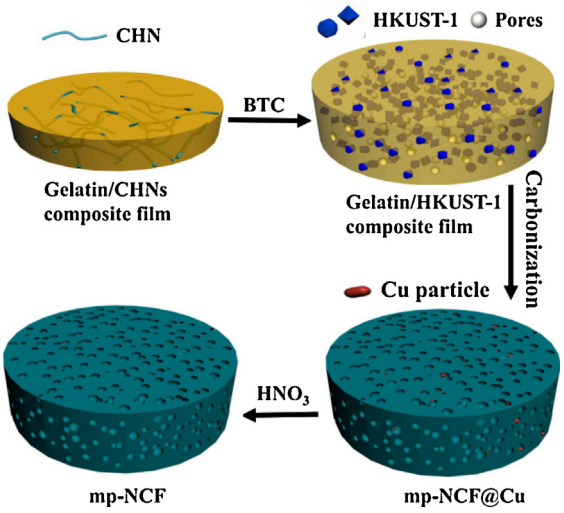

Scheme 1. Schematic illustration of the synthesis process of the mp-NCF from gelatin/CHNs composite films.

skin, type B with 150 blooms, 100–115 free carboxyl groups per 100 g, molecular weight 33 kDa. Copper nitrate ($Cu(NO_3)_2{\cdot}3H_2O$), aminoethanol ($NH_2CH_2CH_2OH$) (AE) and glutaraldehyde (GA) (50 wt%) were obtained from Acros Chemicals. Polycarbonate membranes (PC) (9 cm diameter with 200 nm pores, 11 μm thick and porosity 10%) were purchased from Whatman. Ultrapure water of 18.2 MΩ was produced by a Millipore Direct-Q system.

2.2. Synthesis of free-standing mesoporous nitrogen-doped carbon films

As shown in Scheme 1, CHNs were synthesized by quickly mixing 1.4 mM AE aqueous solution with equal volume of 4 mM $Cu(NO_3)_2$ aqueous solution using a magnetic stirrer, then the mixed solution was aged for 1 or 2 days to form CHNs [24]. A mixture of 4 ml of gelatin aqueous solution (0.1 wt%) and 250 ml CHNs solution was filtered on a PC support (effective diameter 7.2 cm) to form a gelatin/CHNs composite film, and cross-linking by 3 ml 2.5 wt% GA aqueous solution for 1 h. The obtained gelatin/CHNs composite film was peeled off from the support to be free-standing. After that the free-standing gelatin/CHNs composite film was immersed into 10 ml, 10 mM H_3BTC ethanol–water (vol/vol, 1:1) solution at room temperature. After 1 h, a free-standing porous gelatin/HKUST-1 composite film was obtained. Three prepared free-standing gelatin/HKUST-1 composite films were carbonized in a horizontal tube furnace at a rate of 10 °C min^{-1} under argon flow at 600, 800 and 900 °C for 2 h, respectively. Finally, the free-standing and black films were obtained and further immersed into HNO_3 aqueous solution (0.1 M) to remove Cu compounds resulting from HKUST-1, and produced free-standing mesoporous nitrogen-doped carbon films named as mp-NCF-600, mp-NCF-800 and mp-NCF-900, respectively. For comparison, a nitrogen-doped carbon film (g-NCF) was carbonized from pure gelatin film at 600 °C after removing away CHNs from gelatin/CHNs composite film using 10 mM HCl.

2.3. Characterization and electrochemical test

X-ray diffraction (XRD) patterns were recorded by an X'Pert PRO (PANalytical, Netherlands) instrument with Cu Kα radiation at 0.02° steps. The morphologies were investigated using scanning electronic microscopy (SEM) (Hitachi S4800). X-ray photoelectron spectroscopy (XPS) was obtained by an ESCALAB_250Xi X-ray photoelectron spectrometer using Al Kα (λ = 1.5406 Å) X-ray as the excitation source. The nitrogen sorption and desorption measurements were recorded in Micromeritics instrument (ASAP 2020) after activating at 150 °C for 12 h. Fourier transform infrared spectra (FTIR) were recorded by using a Tensor 27 FTIR spectrometer (Bruker Inc.) in the form of KBr pellets. One piece of the prepared mp-NCF film folded into 1 cm × 1 cm (1 mg) and pressed between two pieces of Ni foams (1 cm × 1 cm) and served as electrode for supercapacitor. All electro-chemical tests were carried out by using a CHI 660D (Chenhua Shanghai, China) electrochemical workstation in a 1 M Na_2SO_4 aqueous solution with a platinum counter electrode and a standard calomel reference electrode (SCE).

3. Results and discussion

3.1. Structures and morphology

The XRD results (Fig. 1) indicate the main peaks of the gelatin/HKUST-1 composite film are attributed to the HKUST-1, indicating the CHNs are converted into HKUST-1 in gelatin film (Fig. 1a) [25]. The XRD patterns of both the mp-NCF carbon films converted from gelatin/HKUST-1 composite films at different temperatures and g-NCF film converted from pure gelatin display broad carbon (002) diffraction peak located around 24° (Fig. 1b) [26]. However, before immersing mp-NCF carbon films in 0.1 M HNO_3, several obvious diffraction peaks of Cu crystals are observed apart

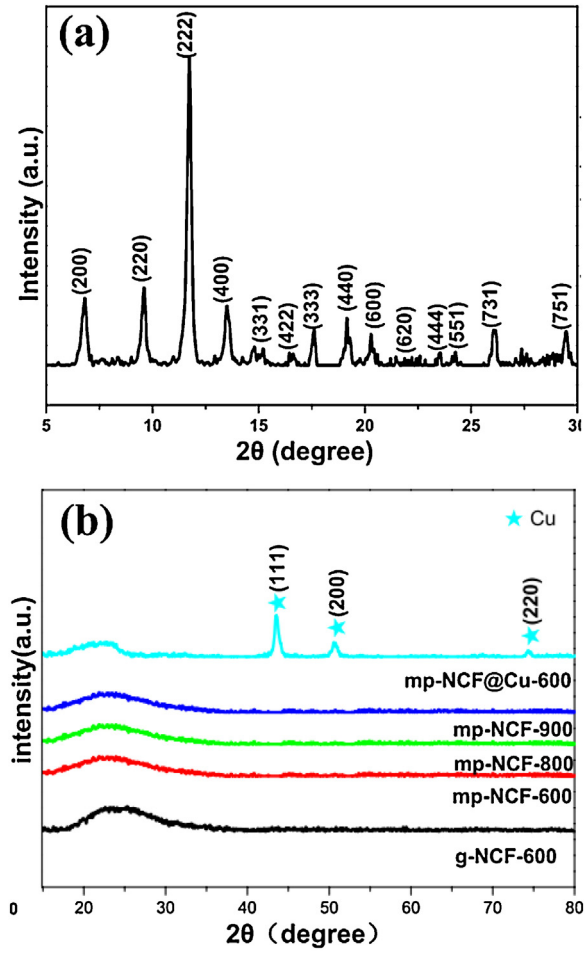

Fig. 1. XRD patterns of (a) gelatin/HKUST-1 composite film, (b) g-NCF-600 (black), mp-NCF-600 (red), mp-NCF-800 (green), mp-NCF-900 (royal blue), mp-NCF@Cu-600 (blue). (For interpretation of the references to color in this figure legend, the reader is referred to the web version of the article.)

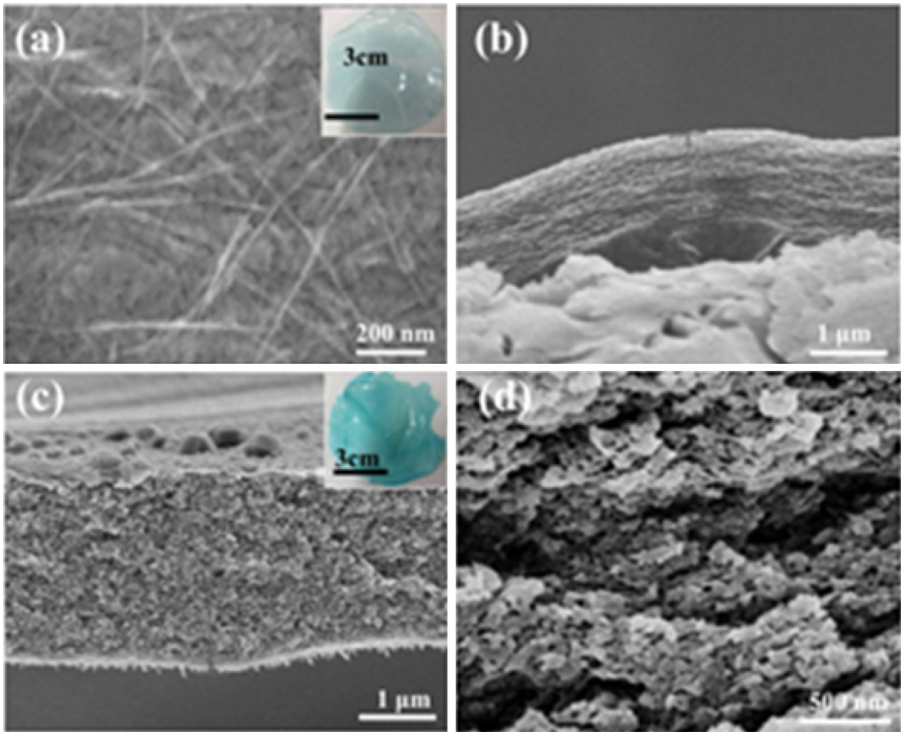

Fig. 2. SEM images of (a) surface and (b) cross section of cross-linked gelatin/CHNs composite film from 4 ml gelatin solution (0.1 wt%) with 250 ml CHNs. (c) and (d) cross-section of gelatin/HKUST-1 composite film converted from (a). The inset in (a) and (c) are the corresponding photos of gelatin/CHNs and gelatin/HKUST-1 thin films, respectively.

from the diffraction of carbon. The Cu crystals in the porous carbon films were the products of the decomposition of HKUST-1 crystals.

The prepared gelatin/HKUST-1 composite film has a thickness of 4.86 μm. Very porous structures are observed in gelatin/HKUST-1 composite film (Fig. 2c and d), which are clearly different from dense gelatin/CHNs film (Fig. 2b). These porous structures and the increment of the thickness are due to the formation of HKUST-1 crystals, which expand the gelatin matrix. Fig. 3a–c shows the morphology of the nitrogen-doped carbon films with Cu particles (mp-NCF@Cu-600) carbonized at 600 °C. It is obvious that pores and Cu particles are observed and distribute uniformly in the film. After removing away Cu particles by HNO_3, the obtained nitrogen-doped carbon film shows abundant pores with diameter of several tens nanometers due to the removal of Cu particles (Fig. 3e and f). The cross-section SEM images indicate that after treatment of HNO_3, the thickness of the film is shrunk to about 2.2 μm. However, the g-NCF film is very dense without obvious mesoporous structures (Fig. S1). Similar porous structures were also observed in the mp-NCF-800 and mp-NCF-900 thin films after removing away Cu particles (Fig. 4). Fig. S2 and Table 1 indicate the pore size and BET surface area of the resulted NCF-600, mp-NCF-800 and NCF-900 are 15 nm and 42.1 $m^2\ g^{-1}$, 20 nm and 58.2 $m^2\ g^{-1}$, and 30 nm and 60.8 $m^2\ g^{-1}$, respectively. It is clear that both the pore size and BET surface area are increased with the carbonization temperature. In addition, the portion of macropores (larger than 50 nm) is also increased.

Fig. 5a shows the corresponding Raman spectra of the gelatin/HKUST-1 and mp-CNF thin films. It is clear that after carbonization, the characteristic D and G peaks of SP^2 carbon are observed. These mean that graphite like carbon is formed. Fig. 5b shows the FTIR spectra of gelatin/HKUST-1 composite film and mp-NCF-600 film, respectively. The strong peak at 1657 cm^{-1} corresponds to the C=O stretching vibration of gelatin and HKUST-1. The double peaks at 1448 and 1378 cm^{-1} are assigned to C–H stretching vibration of aliphatic bridge structure. The absorption peak at 1056 cm^{-1} can be assigned to the stretching vibration of C–O [27,28]. The strong peaks around 1000 cm^{-1} correspond to the out of plane N–H deformation vibrations. The strong peaks around 750 are assigned to Cu–O. The broad peak around 1350 cm^{-1} is assigned to the C=N stretching vibration. From FTIR analysis, the peaks at 2927, 1657, 1448 and 1378 cm^{-1} became weak and disappeared in the mp-NCF film, which confirm the clear conversion of gelatin/HKUST-1 composite film to carbon film.

XPS was employed to characterize the states of nitrogen in the prepared samples (Fig. 6 and Table 1). The survey spectrum

Table 1
Specific surface area and elemental analyses of the samples.

Sample	S_{BET} (m^2/g)	N%	N_1% graphitic quaternary N	N_2% pyrollic N	N_3% amine N	N_4% pyridinic N
Gelatin/HKUST-1	939.7	6.04	–	–	63.2	36.8
g-NCF	2.5	12.1	–	44.7	–	55.3
mp-NCF-600	42.1	11.8	24.9	25.3	–	49.8
mp-NCF-800	58.2	8.9	34.4	25.4	–	40.2
mp-NCF-900	60.8	7.4	40.5	25.6	–	33.9

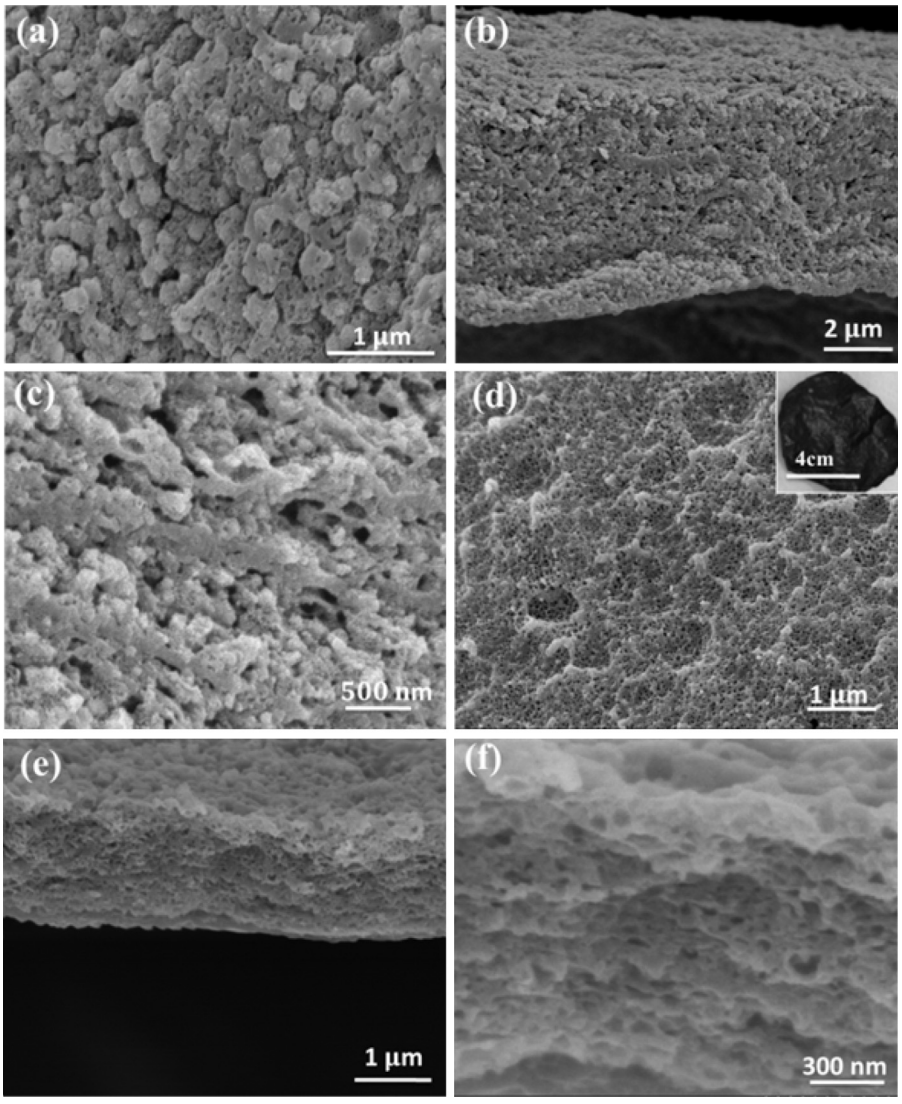

Fig. 3. SEM images of (a) surface and (b) cross section of mp-NCF@Cu-600, (c) higher magnification image of (b); (d) surface, (e) cross section and (f) higher magnification images of mp-NCF-600. The inset in (d) shows its corresponding photo image.

shows the contents of carbon and nitrogen elements within the mp-NCF-600 and mp-NCF-900 are 87.3 at% and 11.8 at%, and 92.3 at% and 7.4 at%, respectively. The high resolution N1s spectra can be deconvoluted into four different signals with binding energies of 400.7, 400.1, 399.6 and 398.6 eV, assigned to graphitic quaternary nitrogen, pyrollic nitrogen, amine nitrogen and pyridinic nitrogen, [29,30] respectively (Fig. 5a–c). For gelatin/CHNs composite film, amine nitrogen was predominant owing to the $-NH_2$ group of gelatin (Fig. 3a). However, for the mp-NCF-600, mp-NCF-900 and g-NCF (Fig. 5b and c), pyrollic nitrogen and pyridinic nitrogen peaks are dominated due to the carbonization. These results indicate that the amine groups are progressively converted to pyrollic nitrogen and pyridinic nitrogen during the carbonization process, as previously found in other materials [15–30]. The corresponding ratio of different N functional groups of mp-NCF-600, mp-NCF-800 and mp-NCF-900 are summarized in Table 1. It is obvious that more graphitic N is formed at higher temperature. This mesoporous nitrogen-doped carbon films are promising for film-like binder-free supercapacitor. The surface area of the mp-NCF-600, mp-NCF-800 and mp-NCF-900 is 42.1, 58.2 and 60.8 $m^2\ g^{-1}$ which is much higher than 2.5 $m^2\ g^{-1}$ of g-NCF-600. The majority of pores are located in the region of mesopores with size of about 20 nm (Fig. S2). But no obvious micropore was detected since no post activation process was conducted.

3.2. Electrochemical performance

The electrochemical performance of the free-standing mp-NCF-600, mp-NCF-800 and mp-NCF-900 in 1 M L^{-1} Na_2SO_4 aqueous electrolytes were evaluated in a three-electrode cell with a Pt counter electrode and a SCE reference electrode. The cyclic voltammetry (CV) curves recorded from g-NCP-600, mp-NCF-600, mp-NCF-800 and mp-NCF-900 at different potential sweep rates are shown in Fig. 7a–d, respectively. The shapes of the CV curves become more and more rectangle when the carbonation temperature is increased. Meanwhile, even for the mp-NCF-900, the rectangle shape CV curve is still with obvious well-broadened peaks. This means pseudocapacitor contributes to the specific capacitor. It is noteworthy that no binder or conductive additives were used for the electrodes preparation. The specific capacitances were calculated according to Ref. [28]. At the sweep rate of 2 mV s^{-1}, the specific capacitances are 158.8, 207.2, 287.5 F g^{-1} for mp-NCF-600, mp-NCF-800 and mp-NCF-900, respectively. While, it is about 47.25 F g^{-1} for g-NCF sample. The mp-NCF thin film

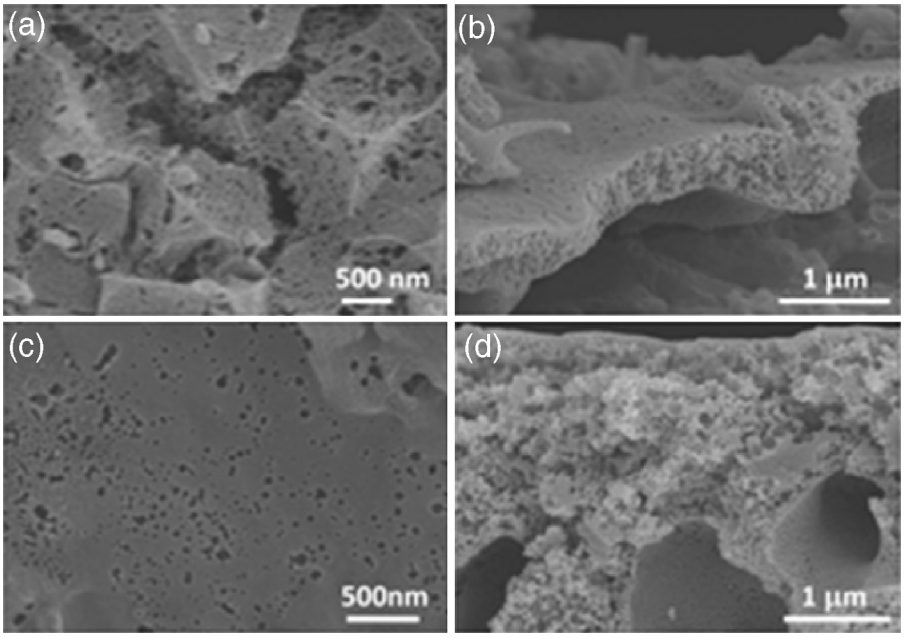

Fig. 4. SEM images of (a) surface and (b) cross section of mp-NCF-800, (c) surface and (d) cross section of mp-NCF-900.

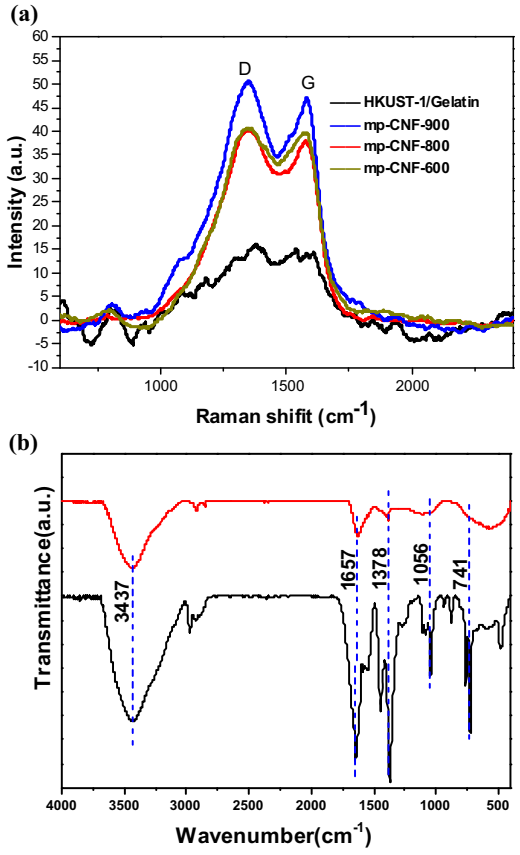

Fig. 5. (a) Raman spectra of the as-prepared mp-NCF-600 thin films carbonized at different temperatures, (b) FTIR spectra of gelatin/HKUST-1 (black) and mp-NCF-600 (red), respectively. (For interpretation of the references to color in this figure legend, the reader is referred to the web version of the article.)

exhibits much higher specific capacitance than g-NCF due to their large BET surface area and mesoporous structures [9].

Galvanostatic charge/discharge between −0.9 and 0 V were employed to estimate the electrochemical performance of mp-NCF samples as electrode for supercapacitor (Fig. 8a–c). The galvanostatic charge/discharge curves of mp-NCF-600 and mp-NCF-800 are not very symmetric. We anticipate it may be due to the relative low carbonization temperature resulting poor electrical conductivity and remaining functional groups [31]. While, more symmetrical curves are observed for mp-NCF-900 electrode. These results are in agreement with the CV curves (Fig. 7). These slight deviations of both CV and V–t curves indicate the presence of a pseudocapacitance effect. [12,32–35] Specific capacitance of each electrodes were calculated according to $C = I \times \Delta t/(\Delta V \times m)$, where I is the discharge current, Δt is the discharge time from −0.8 to 0 V, ΔV is the voltage difference within the discharge time, and m is the mass of active materials. The specific capacitances for the mp-NCF thin film at 5.0 A g^{-1} current density are calculated to be 19.6, 143.5, 126.3 and 168 F g^{-1} for g-CNF-600, mp-NCF-600, mp-NCF-800 and mp-NCF-900 electrodes, respectively. The capacitance of mp-NCF electrodes is very close to those of reported various carbon based electrodes [9,12,15,27,31–35]. It is well known that carbon materials with high surface area and micropores have been typically generated through complex activation by NaOH/KOH et al. at high temperature [32,35]. But Zhao reported that the higher the surface area the bigger the specific capacitance is not always true [12]. Especially, when pseudocapacitor is occurred, for example in the nitrogen-doped porous carbon, microporous may prohibit the access of the electrolyte to reach the surface and process the reaction. But in our case, the mesoporous could make electrolyte more easy access and promote the reaction. Therefore, both the mesoporous feature of the mp-NCF provides free and quick access of electrolyte and ions, and the nitrogen-doping species resulted pseudocapacitance contributes to the high electrochemical performance.

The mp-NCF-900 demonstrates the best performance of specific capacity of 316 F g^{-1} at a current density of 0.5 A g^{-1}. The durability of the mp-NCF-900 electrode was evaluated by the long-term charge/discharge behavior. Fig. 8d displays the capacitance of the mp-NCF-900 at a current density of 5 A g^{-1}. The capacitance still remains at 156.2 F g^{-1} after 11,000 cycles with degrading rate of 0.00064% per cycle, which clearly displays a good cycling stability of mp-NCF-900 as supercapacitve electrode material.

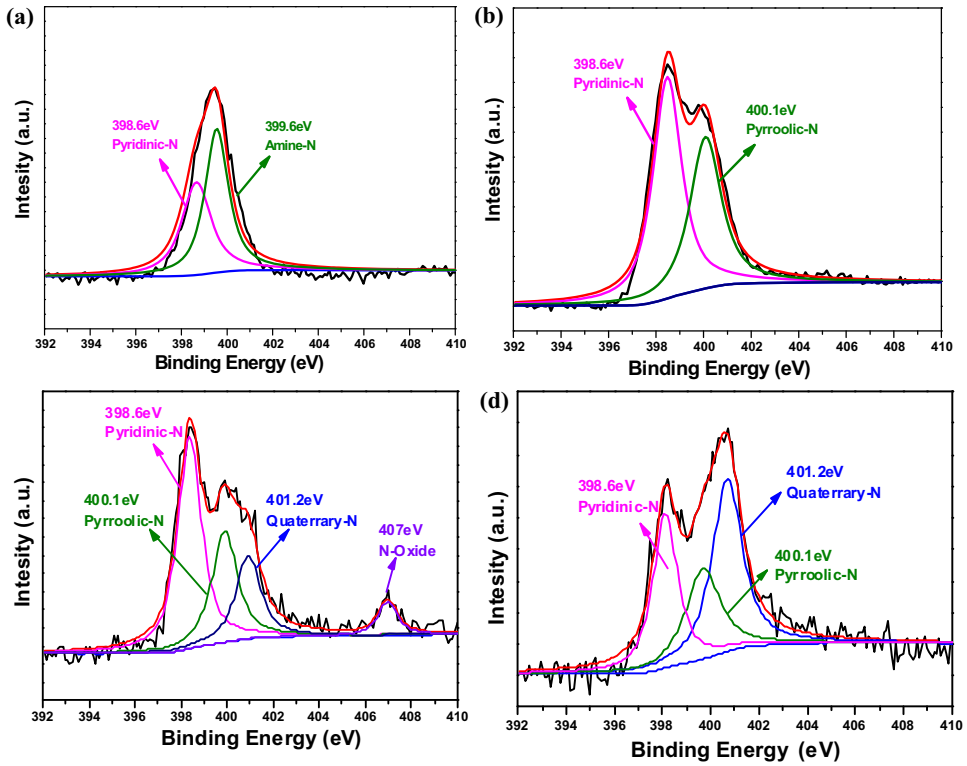

Fig. 6. N1s XPS spectra of (a) gelatin/CHNs composite films, (b) g-NCF, (c) mp-NCF-600, (d) mp-NCF-900.

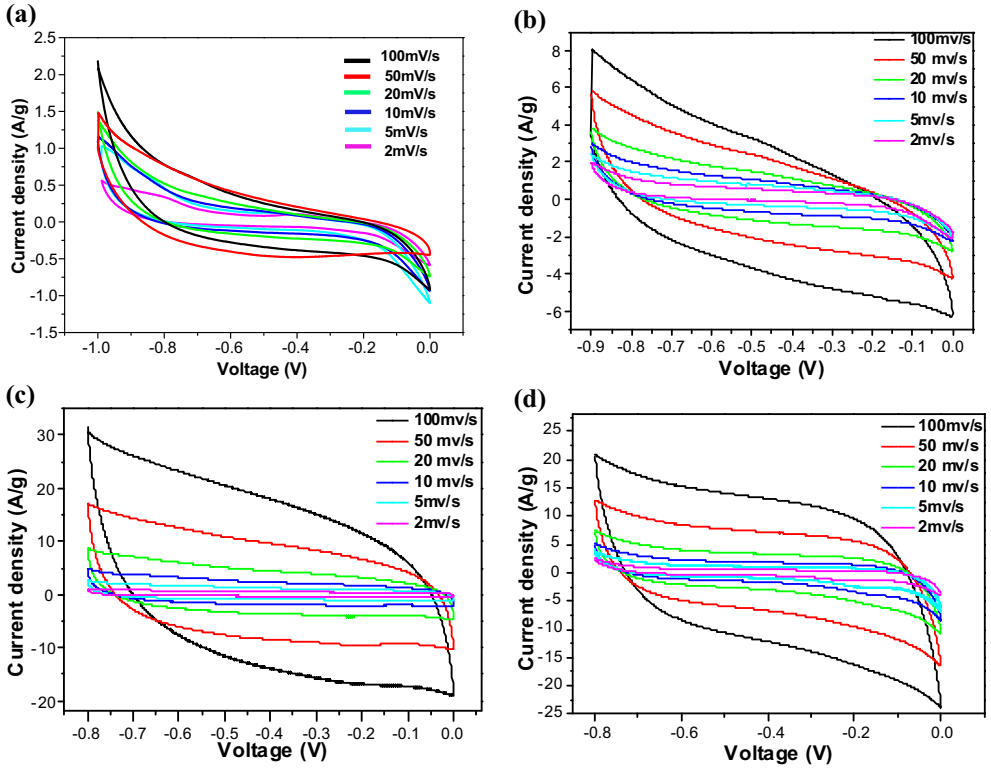

Fig. 7. (a–d) CV curves of the g-NCF, mp-NCF-600, mp-NCF-800 and mp-NCF-900 at different scan rates in 1 M Na_2SO_4 aqueous solution respectively.

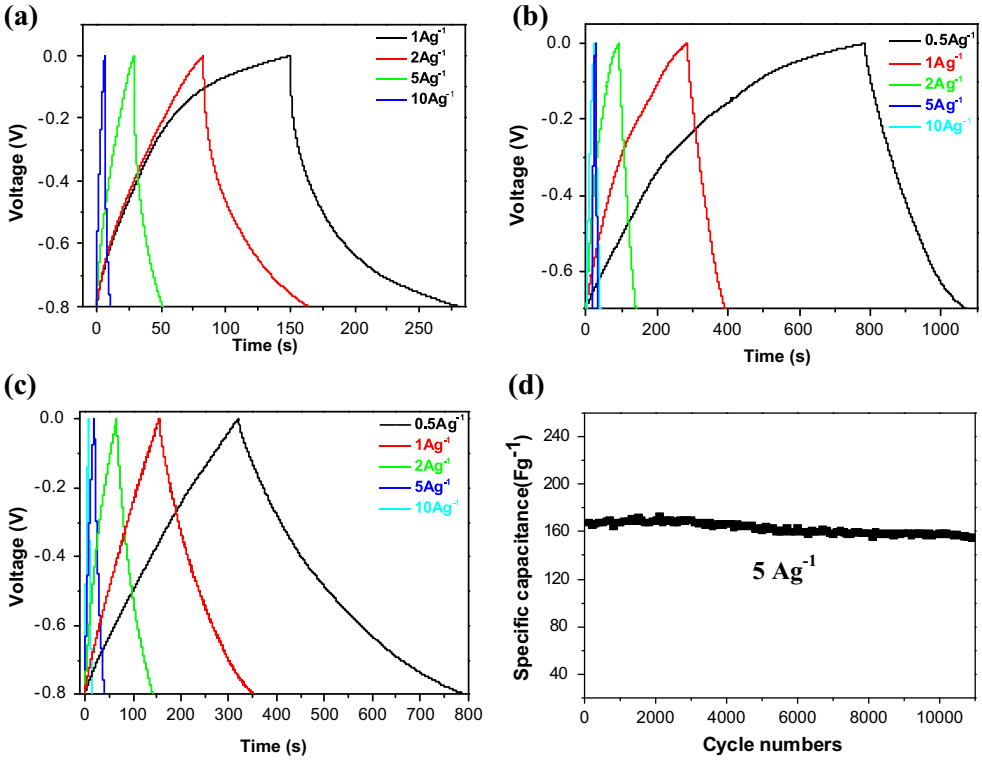

Fig. 8. (a–c) GV constant-current charge–discharge performance of the g-NCF, mp-NCF-600, mp-NCF-800 and mp-NCF-900 in 1 M Na_2SO_4 aqueous solution, respectively. (d) Cycling stability of mp-NCF-900 at current density of 5 A g^{-1}.

4. Conclusion

In summary, free-standing mesoporous nitrogen-doped carbon films (mp-NCF) were prepared by carbonization of porous gelatin/HKUST-1 composite films and removing away copper compounds. The mp-NCF thin film was directly used as electrode for capacitors without binder or conductive additive. In 1 M Na2SO4 electrolyte solution, the mp-NCF-900 electrode exhibited high capacitance of 168 F g^{-1} at 5 A g^{-1}, and long cycling stability. The capacitance still remains at 156.2 F g^{-1} after 11,000 cycles with degrading rate of 0.00064% per cycle. Although this value is close to the capacitance reported so far for many carbon-based materials, the carbon electrode in our work is free-standing nitrogen-doped carbon film, which is an alternative candidate for film-like capacitors.

Acknowledgements

This work was supported by the National Basic Research Program of China 973 Program (2015CB655302), Natural Science Foundation for Zhejiang Province Science Fund for Distinguished Young Scholars (LR14E020001) and the National Natural Science Foundations of China (NSFC 21271154, U1537109).

Appendix A. Supplementary data

Supplementary data associated with this article can be found, in the online version, at doi:10.1016/j.apmt.2016.08.001.

References

[1] Y. Xia, R. Mokaya, Synthesis of ordered mesoporous carbon and nitrogen-doped carbon materials with graphitic pore walls via a simple chemical vapor deposition method, Adv. Mater. 16 (2004) 1553–1558.
[2] T.V. Vineesh, M.A. Nazrulla, S. Krishnamoorthy, T.N. Narayanan, S. Alwarappa, Synergistic effects of dopants on the spin density of catalytic active centres of N-doped fluorinated graphene for oxygen reduction reaction, Appl. Mater. Today 1 (2015) 74–79.
[3] R. Giardi, S. Porro, T. Topuria, L. Thompson, C.F. Pirri, H.-C. Kim, One-pot synthesis of graphene-molybdenum oxide hybrids and their application to supercapacitor electrodes, Appl. Mater. Today 1 (2015) 27–32.
[4] A. Suryawanshi, M. Biswal, D. Mhamane, P. Yadav, A. Banerjee, P. Yadav, S. Patil, V. Aravindan, S. Madhavi, S. Ogale, A comparative evaluation of differently synthesized high surface area carbons for Li-ion hybrid electrochemical supercapacitor application: Pore size distribution holds the key, Appl. Mater. Today 2 (2016) 1–6.
[5] 9 R. Giardi, S. Porro, T. Topuria, L. Thompson, C. Fabrizio Pirri, H.-C.L. Kim, One-pot synthesis of graphene-molybdenum oxide hybrids and their application to supercapacitor electrodes, Appl. Mater. Today 1 (2015) 27–32.
[6] Z.X. Yang, Y.D. Xia, R. Mokaya, Enhanced hydrogen storage capacity of high surface area zeolite-like carbon materials, J. Am. Chem. Soc. 129 (2007) 1673–1679.
[7] J.H. Knox, B. Kaur, G.R. Millward, Structure and performance of porous graphitic carbon in chromatography, J. Chromatogr. A 352 (1986) 3–25.
[8] J.R. -Mirasol, T. Cordero, L.R. Radovic, J.J. Rodriguez, Structural and textural properties of pyrolytic carbon formed within a microporous zeolite template, Chem. Mater. 10 (1998) 550–558.
[9] A.-H. Lu, W.-C. Li, W. Schmidt, W. Kiefer, F. Schüth, Easy synthesis of an ordered mesoporous carbon with a hexagonally packed tubular structure, Carbon 42 (2004) 2939–2948.
[10] S. Yoon, J. Lee, T. Hyeon, S.M. Oh, Electric double-layer capacitor performance of a new mesoporous carbon, J. Electrochem. Soc. 147 (2000) 2507–2512.
[11] J. Kim, M. Choi, R. Ryoo, Synthesis of mesoporous carbons with controllable N-content and their supercapacitor properties, Bull. Korean Chem. Soc. 29 (2008) 413–416.
[12] Q. Shi, R. Zhang, Y. Lv, Y. Deng, A.A. Elzatahrya, D. Zhao, Nitrogen-doped ordered mesoporous carbons based on cyanamide as the dopant for supercapacitor, Carbon 84 (2015) 335–346.
[13] D. Wang, F. Li, L. Yin, X. Lu, Z.-G. Chen, I.R. Gentle, G.Q. Lu, H.-M. Cheng, Nitrogen-doped carbon monolith for alkaline supercapacitors and understanding nitrogen-induced redox transitions, Chem. Eur. J. 18 (2012) 5345–5351.
[14] J. Wei, D. Zhou, Z. Sun, Y. Deng, Y. Xia, D. Zhao, A controllable synthesis of rich nitrogen-doped ordered mesoporous carbon for CO_2 capture and supercapacitors, Adv. Funct. Mater. 23 (2013) 322–2328.
[15] L. Song, Z. Liu, A.L.M. Reddy, N.T. Narayanan, J.T. -Tijerina, J. Peng, G.H. Gao, J. Lou, R. Vajtai, P.M. Ajayan, Binary and ternary atomic layers built from carbon, boron, and nitrogen, Adv. Mater. 24 (2012) 4878–4895.

[16] M.J. Zhi, C.C. Xiang, J.T. Li, M. Li, N.Q. Wu, Nanostructured carbon–metal oxide composite electrodes for supercapacitors: a review, Nanoscale 5 (2013) 72–78.
[17] B. Qiu, B.C. Lin, L.H. Qiu, F. Yan, Alkaline imidazolium- and quaternary ammonium-functionalized anion exchange membranes for alkaline fuel cell applications, J. Mater. Chem. 22 (2012) 1040–1045.
[18] W.Z. Shen, W.B. Fan, Nitrogen-containing porous carbons: synthesis and application, J. Mater. Chem. A 1 (2013) 999–1013.
[19] L. Shi, H.B. Huang, L.W. Sun, Y.P. Lu, B.Y. Du, Y.Y. Mao, J.W. Li, Z.Z. Ye, X.S. Peng, $Fe(CN)_6]^{4-}$ decorated mesoporous gelatin thin films for colorimetric detection and adsorbent of heavy metal ions, Dalton Trans. 42 (2013) 13266–13272.
[20] X.Y. Chen, C. Chen, Z.J. Zhang, D.H. Xie, Gelatin-derived nitrogen-doped porous carbon via a dual-template carbonization method for high performance supercapacitors, J. Mater. Chem. A 1 (2013) 10903–10911.
[21] G.P. Mane, S.N. Talapaneni, C. Anand, S. Varghese, H. Iwai, Q. Ji, K. Ariga, T. Mori, A. Vinu, Preparation of highly ordered nitrogen-containing mesoporous carbon from a gelatin biomolecule and its excellent sensing of acetic acid, Adv. Funct. Mater. 22 (2012) 3596–3604.
[22] E.R. -Hitzky, M. Darder, F.M. Fernandes, E. Zatile, F.J. Palomares, P. Aranda, Supported graphene from natural resources: easy preparation and applications, Adv. Mater. 23 (2011) 5250–5255.
[23] B. Xu, S. Hou, G. Cao, F. Wu, Y.S. Yang, Sustainable nitrogen-doped porous carbon with high surface areas prepared from gelatin for supercapacitors, J. Mater. Chem. 22 (2012) 19088–19093.
[24] H.W. Huang, Q. Yu, X.S. Peng, Z.Z. Ye, Mesoporous protein thin films for molecule delivery, J. Mater. Chem. 21 (2011) 13172–13179.
[25] Y.Y. Mao, W. Cao, J.W. Li, Y. Liu, Y.L. Ying, L.W. Sun, X.S. Peng, Enhanced gas separation through well-intergrown MOFs membranes: seeds morphology and crystal growth habit effects, J. Mater. Chem. A 1 (2013) 11711–11716.
[26] J. Hu, H.L. Wang, Q.M. Gao, H.L. Guo, Carbon 48 (2010) 3599.
[27] L. Liu, Q.-F. Deng, X.-X. Hou, Z.-Y. Yuan, User-friendly synthesis of nitrogen-containing polymer and microporous carbon spheres for efficient CO_2 capture, J. Mater. Chem. 22 (2012) 15540–15548.
[28] Y. Liu, Y.L. Ying, Y.Y. Mao, L. Gu, Y.W. Wang, X.S. Peng, CuO nanosheets/rGO hybrid lamellar films with enhanced capacitance, Nanoscale 5 (2013) 9134–9140.
[29] W.-H. Lee, J.H. Moon, Monodispersed N-doped carbon nanospheres for supercapacitor application, ACS Appl. Mater. Interfaces 6 (2014) 13968–13976.
[30] N.P. Wickramaratne, J. Xu, M. Wang, L. Zhu, L.M. Dai, M. Jaroniec, Nitrogen enriched porous carbon spheres: attractive materials for supercapacitor electrodes and CO_2 adsorption, Chem. Mater. 26 (2014) 2820–2828.
[31] B. Liu, H. Shioyam, H.L. Jiang, X.B. Zhang, Q. Xu, Metal–organic framework (MOF) as a template for syntheses of nanoporous carbons as electrode materials for supercapacitor, Carbon 48 (2010) 456–463.
[32] B. Xu, S. Hou, G. Cao, F. Wu, Y. Yang, Sustainable nitrogen-doped porous carbon with high surface area prepared from gelatine for supercapacitors, J. Mater. Chem. 22 (2012) 19088–19093.
[33] J.-W. Jeon, R. Sharma, P. Meduri, B.W. Arey, H.T. Schaef, J.L. Lutkenhaus, J.P. Lemmon, P.K. Thalapally, M.I. Nandasiri, B.P. McGrail, S.K. Nune, In situ one-step synthesis of hierarchical nitrogen-doped porous carbon for high performance supercapacitors, ACS Appl. Mater. Interfaces 6 (2014) 7214–7222.
[34] X. Chen, C. Chen, Z.J. Zhang, D.H. Xie, Gelatin-derived nitrogen doped porous carbon via a dual-templated carbonization method for high performance supercapacitors, J. Mater. Chem. A 1 (2013) 10903–10911.
[35] J.-S. Wei, H. Ding, Y.-G. Wang, H.-M. Xiong, Hierarchical porous carbon materials with high capacitance derived from Schiff-base networks, ACS Appl. Mater. Interfaces 7 (2015) 5811–5819.